NUMERICAL INVESTIGATION OF TURBULENCE MODELS FOR SIMULATION OF A GAS-LIQUID STIRRED TANK

YEFEI LIU
College of Chemical Engineering, Nanjing Tech University, yefei.liu@njtech.edu.cn

Keywords: *Stirred tank; CFD; two-fluid model; k-ε model; OpenFOAM*

1. Introduction

Gas-liquid stirred tank reactors are widely used in chemical, biochemical and petrochemical industries. The interaction between stationary baffles and rotating impellers produces complicated and highly turbulent flow, which in turn has substantial influence on gas holdup, bubble size distribution and interphase transfer efficiency. It is very important to understand the gas-liquid turbulence in stirred tanks for successful reactor design and scale-up.

During last decades computational fluid dynamics (CFD) methods have been developed for resolving turbulent hydrodynamics in gas-liquid stirred tanks. In the simulation of gas-liquid stirred tanks, due to the simplicity, the *k-ε* model is usually the preferable choice to simulate the liquid turbulence. Among the various formulations of the *k-ε* models (standard, RNG and realizable), the standard model has been most widely used. The realizable *k-ε* model was also employed for simulating the gas-liquid hydrodynamics and mass transfer in stirred tanks. The predictions of liquid velocity, local bubble sizes and dissolved oxygen concentration were in good agreement with experimental data reported in the literature. However, there is currently no clear justification on the choice of different formulations of *k-ε* models for simulating gas-liquid stirred tanks.

The purpose of this work is to provide detailed investigation on the turbulence modelling in simulating of a gas-liquid stirred tank. Also, the previous studies in the literature are performed in different commercial CFD tools. The other objective of this work is to make the validation of the open source CFD tool OpenFOAM, which has been not done until the date for gas-liquid stirred tanks. The simulation results are compared with the data in the literature. The different formulations of *k-ε* models are more specifically investigated and the influence of bubble-induced turbulence is also evaluated by the comparison with the liquid turbulent kinetic energy.

2. Mathematical models

The CFD simulation is performed with the two-fluid model. The continuity and momentum equations of the gas and liquid phases are written as

$$\frac{\partial(\alpha_k\rho_k)}{\partial t}+\nabla\cdot(\alpha_k\rho_k\mathbf{U}_k)=0 \tag{1}$$

$$\frac{\partial(\alpha_k\rho_k\mathbf{U}_k)}{\partial t}+\nabla\cdot(\alpha_k\rho_k\mathbf{U}_k\mathbf{U}_k)=-\alpha_k\nabla p+\nabla\cdot(\alpha_k\tau_k)+\alpha_k\rho_k\mathbf{g}+\mathbf{F}_k+\mathbf{M}_k \tag{2}$$

where *k* refers to the phase (*l* for liquid and *g* for gas), **U** is the phase velocity, α is the volume fraction of each phase, $\boldsymbol{\tau}$ is the effective stress tensor, $\mathbf{M}_k$ is the interfacial momentum transfer term due to various interphase forces. The term **F** represents the Coriolis and centrifugal forces expressed in the MRF method for rotating flows and it is calculated as

$$\mathbf{F}_k=-\boldsymbol{\Omega}\times\left(\alpha_k\rho_k\mathbf{U}_k\right) \tag{3}$$

where $\boldsymbol{\Omega}$ is the angular velocity vector.

In this study the only drag is considered, while the other forces are neglected since they have little effect on the flows. The momentum interfacial transfer term due to the drag force is calculated as

$$\mathbf{M}_{D,g}=-\mathbf{M}_{D,l}=\frac{3}{4}\alpha_g\rho_l\frac{C_D}{d_b}\left|\mathbf{U}_g-\mathbf{U}_l\right|\left(\mathbf{U}_l-\mathbf{U}_g\right) \tag{4}$$

where d_b is the mean bubble size and C_D is the drag coefficient determined by the flow regime and the liquid property. Here the drag coefficient follows the model proposed by Khopkar et al. [8] as

$$\frac{C_D-C_{D0}}{C_{D0}}=K\left(\frac{d_b}{\lambda}\right)^3 \tag{5}$$

where λ is the Kolmogorov scale, K is an empirical constant, $K = 6.5\times 10^{-6}$, C_{D0} is drag coefficient for a single bubble rising in a stagnant liquid and it is estimated as

$$C_{D0}=\max\left[\frac{24}{\mathrm{Re}}\left(1+0.15\,\mathrm{Re}^{0.687}\right),\ \frac{8}{3}\frac{\mathrm{Eo}}{\mathrm{Eo}+4}\right] \tag{6}$$

where the bubble Reynolds number Re and Eötvös number Eo are defined as

$$\mathrm{Re} = \frac{\rho_l d_b \left|\mathbf{U}_g - \mathbf{U}_l\right|}{\mu_l} \tag{7}$$

$$\mathrm{Eo} = \frac{g\left(\rho_l - \rho_g\right) d_b^2}{\sigma} \tag{8}$$

The *k-ε* models with three formulations (standard, RNG, and realizable) are implemented with the two-fluid model.

3. Numerical simulation

Nowadays the open source CFD tool OpenFOAM gains some success in the multiphase flow simulation. The OpenFOAM package offers the possibility to have insight into the source codes and hence it is of great convenience to implement various physical models. In this work, the two-phase flow solver is developed based on the `twoPhaseEulerFoam` solver in OpenFOAM-2.3.1. Our solver is rewritten into the incompressible version, since the compressibility is quite small in the simulation. The effect of phase inversion has been treated using the blending methods. The different formulations of *k-ε* turbulence models for liquid turbulence are implemented into the solver.

The linear equation systems resulting from the finite volume discretization are solved in a segregated fashion. The pressure-velocity coupling is handled using the PISO solution algorithm. The interphase coupling terms in the phase momentum equations are treated using the semi-implicit method. First, the gas phase fraction equation is solved. Second, the pressure equation is constructed from the continuity equations and solved. Third, the predicted phase velocities are corrected by the new pressure fields.

The gas-liquid flow generated by the six-bladed down-pumping pitched-blade turbine in a stirred tank is simulated. The diameter of the cylindrical vessel is T = 0.19 m. More details of the configuration can be found in Aubin et al.[1]. The vessel is filled with water and air is supplied at the volumetric gas flow rate of 4.29×10^{-5} m^3/s. The mean bubble size of 4 mm is used in this work. The impeller rotational speed is equal to 300 rpm. Differently from the work of Khopkar et al. [2], the whole geometry of the stirred vessel is considered as the computational domain. By using the MRF method, the computational domain is divided into two cell zones, one for the rotating reference frame and the other for the stationary reference frame.

Initially, the static water exists in the stirred tank and the gas holdup is set to be zero within the static water. The gas distributor is treated as a uniform inlet with the gas volume fraction of 1.0. The liquid inlet velocity is set to zero for all test cases because of no water supply into the stirred tank. The pressure at the inlet is specified using the zero gradient boundary condition. At the outlet, the pressure is specified as atmospheric pressure. The no-slip boundary condition is applied at the wall for the velocities of gas and liquid phases. The standard wall function is used to specify the turbulence quantities. The transient solutions are performed for 20 s and the time-averaged results are obtained using the field averaging utility.

4. Results and discussion

Figure 1 shows the predicted profiles of liquid axial velocity using three *k-ε* models. The three models give very close results at the axial position z/T = 0.31, but the agreement with experimental data is still not obtained. The flow fields predicted using the three *k-ε* models are shown in Figure 2. It can be seen that similar results are found between the standard and RNG models. Differently, in the upper region of the vessel, the higher liquid velocity is predicted using the realizable model.

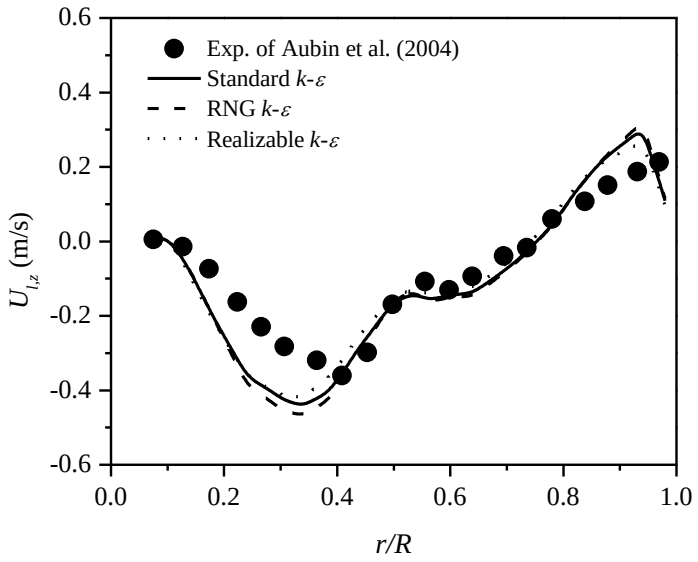

Figure 1: Comparison of liquid axial velocity predicted using three *k-ε* models.

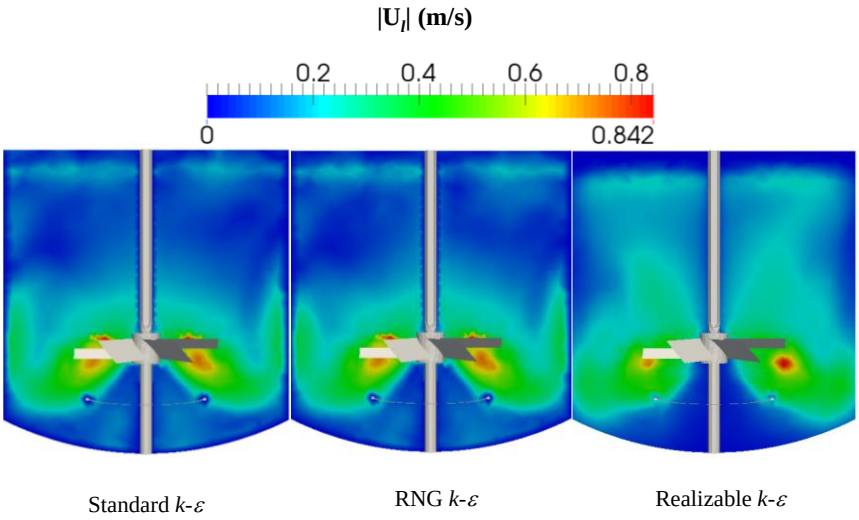

Figure 2: Comparison of liquid velocity fields predicted using three *k*-*ε* models.

Figure 3 gives the profiles of liquid turbulence quantities predicted using the three *k*-*ε* models. In Figure 3(a), the overprediction on turbulent kinetic energy is also provided by the realizable model. Although the peak in turbulent kinetic energy is underpredicted by the RNG model, good agreement with experimental data is found at the other radial positions. Comparing with the standard and realizable models, the RNG model gives smaller values of turbulent kinetic energy. The RNG model is more responsive to the effects of rapid strain than the standard model. In the rapid strained flows, the RNG model predicts a lower turbulent viscosity than the standard model, as shown in Figure 3(c).The turbulence production term becomes smaller and thus the turbulent kinetic energy is reduced.

In Figure 3(b), the smaller values of the dissipation rate of turbulent kinetic energy are also observed for the RNG model, which is due to the smaller turbulence production term in the transport equation of dissipation rate. In Figure 3(c), a different profile of liquid turbulent kinematic viscosity is predicted using the realizable model and the largest value is observed near the impeller blade tip (r/R = 0.5). It was reported that the realizable model has a limitation that it produces non-physical turbulent viscosity in the situations when the computational domain is composed of both rotating and stationary zones. Therefore, great caution should be given when using the realizable model to predict the turbulent viscosity.

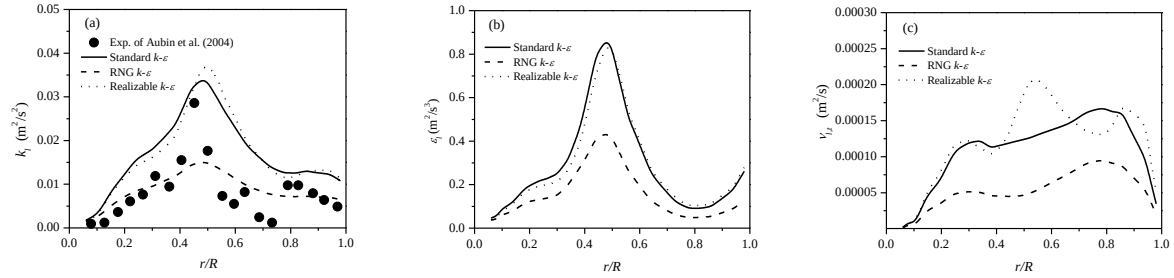

Figure 3: Comparison of liquid turbulent kinetic energy (a), dissipation rate (b) and turbulent kinematic viscosity (c) predicted using three *k*-*ε* models.

Acknowledgements

The financial support from the National Natural Science Foundation (21606124) is gratefully acknowledged. The authors thank all those involved in the organisation of OFW13 and to all the contributors that will enrich this event.

References

[1] Aubin, J., Le Sauze, N., Bertrand, J., Fletcher, D. F., Xuereb, C., 2004. PIV measurements of flow in an aerated tank stirred by a down- and an up-pumping axial flow impeller. Exp. Therm. Fluid Sci. 28, 447-456.

[2] Khopkar, A. R., Aubin, J., Xuereb, C., Le Sauze, N., Bertrand, J., Ranade, V. V., 2003. Gas-liquid flow generated by a pitched-blade turbine: Particle image velocimetry measurements and computational fluid dynamics simulations. Ind. Eng. Chem. Res. 42, 5318-5332.